levels of MUV increase photoinhibition and that excluding MUV decreases photoinhibition in ^{14}C productivity measurements.

A quantitative analysis of our data (*4*), shows that the biological weighting function for photoinhibition of chloroplasts (*11*) allows calculation of a biologically effective dose which is consistent with the measured photoinhibition. This postulated relative biological efficiency for photoinhibition (PI), $\epsilon_{PI}(\lambda)$, is shown in Fig. 1 where we have included the DNA action spectrum (*12*), $\epsilon_{DNA}(\lambda)$, for comparison.

A distinguishing feature of $\epsilon_{PI}(\lambda)$ is that, while it has a maximum in the MUV, it continues into the visible region of the spectrum. For surface irradiance [$E_d(\lambda)$ in Fig. 1], a quantitative evaluation shows (*4*) that 25 percent of the photoinhibition weighted dose is due to radiation below 340 nm (the MUV region), 50 percent of this dose is due to radiation below 390 nm, and the remainder is due to wavelengths longer than 390 nm. In contrast, biologically effective doses, for photoprocesses such as $\epsilon_{DNA}(\lambda)$, are completely due to radiation in the MUV region of the spectrum.

In Fig. 1 we have also plotted downward spectral irradiance for two stratospheric ozone thicknesses (*13*). The effect of a diminished ozone thickness is to cause an increase in the irradiance at the ocean surface in the MUV region. The potential biological impact of this increased MUV is dependent on $\epsilon(\lambda)$, as manifest in the respective amplification factor. In Fig. 2 we have plotted the radiation amplification factor, R, versus stratospheric ozone thickness for $\epsilon_{PI}(\lambda)$ and $\epsilon_{DNA}(\lambda)$ (*14*). These curves show that R is approximately 0.1 for photoinhibition, while it ranges between 2 and 4 for photoprocesses weighted by $\epsilon_{DNA}(\lambda)$. Thus the radiation amplification factor is 20 to 40 times larger for ϵ_{DNA} than for ϵ_{PI}.

If we accept the hypothesis that $\epsilon_{PI}(\lambda)$ adequately describes the spectral weighting of photoinhibition and the effects of excluded and enhanced MUV on phytoplankton photosynthesis, as measured by the static bottle ^{14}C technique, then we can draw the following conclusions and observations: (i) possible changes in the stratospheric ozone thickness will cause only small changes in the biologically effective photoinhibition dose, E_{PI} (since $R_{PI} < 0.1$); (ii) even if the biological amplification factor, for a photoinhibition change in photosynthesis, is as large as our estimate of 5, the total amplification factor for a change in photosynthesis (ϵ_{PI} weighted) due to a change in ozone will be less than 1; (iii) if photoprocesses other than photoinhibition can potentially affect natural phytoplankton populations (for example, MUV absorption and damage to DNA, which may not become evident for incubation times that are short compared to times of cell division), then the relevant $\epsilon(\lambda)$ for these alternative photoprocesses must be identified in order to estimate possible detrimental effects of increased MUV; (iv) photoprocesses having relative biological efficiencies weighted toward the MUV region of the spectrum (for example, ϵ_{DNA}) have amplification factors greater than unity which, when coupled with biological amplification factors greater than unity, gives them the potential for significant biological impact with increased MUV; and (v) conclusions regarding the possible impact of reduced ozone, hence enhanced MUV, with the use of this technique are limited since the present ^{14}C technique is not adequate to assess photoprocesses having a time frame longer than the limited incubation period of this method.

RAYMOND C. SMITH
KAREN S. BAKER
Visibility Laboratory, Scripps Institution of Oceanography, University of California, San Diego, La Jolla 92093

References and Notes

1. N. G. Jerlov, *Nature (London)* **166**, 111 (1950); J. Lenoble, *Ann. Geophys.* **12**, 16 (1956); P. Halldal and O. Taube, in *Photophysiology*, A. C. Giese, Ed. (Academic Press, New York, 1972), vol. 7, pp. 163–188.
2. R. C. Smith and K. S. Baker, *Photochem. Photobiol.* **29**, 311 (1979).
3. Environmental Studies Board, *Biological Impacts of Increased Intensities of Solar UV Radiation* (National Academy of Sciences–National Academy of Engineering, Washington, D.C., 1973); D. S. Nachtwey *et al.* Eds., Climatic Impact Assessment Program (CIAP), *Impacts of Climate Changes in the Biosphere*, CIAP Monograph 5, part 1, *Ultraviolet Radiation Effects*, Department of Transportation, DOT-TST-75-44 (1975) (available from National Technical Information Service, Springfield, Va.); J. C. Calkins and D. S. Nachtwey, in *ibid.*, pp. 5-3 to 5-8; C. Lorenzen, in *ibid.*, pp. 5-81 to 5-91.
4. R. C. Smith, K. S. Baker, O. Holm-Hansen, R. Olsen, *Photochem. Photobiol.*, in press.
5. National Research Council, *Stratospheric Ozone Depletion by Halocarbons: Chemistry and Transport* (National Academy of Sciences, Washington, D.C., 1979); ——, *Protection Against Depletion of Stratospheric Ozone by Chlorofluorocarbons* (National Academy of Sciences, Washington, D.C., 1979).
6. J. E. McDonald, statements submitted before the House Subcommittee on Transportation Appropriations, 2 March 1971.
7. A. E. S. Green, G. B. Findley, Jr., K. F. Klenk, W. M. Wilson, T. Mo, *Photochem. Photobiol.* **24**, 353 (1976); R. D. Rundel and D. S. Nachtwey, *ibid.* **28**, 345 (1978).
8. J. D. H. Strickland and T. R. Parsons, *A Practical Handbook of Seawater Analysis* (Fisheries Research Board of Canada, Ottowa, 1968); R. W. Eppley and J. D. H. Strickland, *Adv. Microbiol. Sea* **1**, 23 (1968).
9. G. P. Harris, *Arch. Hydrobiol. Beihett* **10**, 1 (1978), and references therein.
10. E. Steeman-Nielsen, *J. Cons. Int. Expl. Mer* **29**, 130 (1964); V. Ilmavirta and I. Hakala, *Ann. Bot. Fenn.* **9**, 77 (1972); H. R. Jitts, A. Morel, Y. Saijo, *Aust. J. Mar. Freshwater Res.* **27**, 441 (1976); C. Lorenzen, in (*3*).
11. L. W. Jones and B. Kok, *Plant Physiol.* **41**, 1037 (1966).
12. R. B. Setlow, *Proc. Natl. Acad. Sci. U.S.A.* **71**, 9, 3363 (1974).
13. Calculated with the use of the model of A. E. S. Green *et al.* (*15*) as reparameterized for a marine atmosphere by K. S. Baker, R. C Smith, and A. E. S. Green (*Photochem. Photobiol.*, in press) using an ozone thickness of 0.32 atm · cm.
14. Calculated (*13*) using an instantaneous dose rate (for noon in June at 32°N). Comparison of R values, based on a yearly biological dose, would not qualitatively alter our conclusions.
15. A. E. S. Green, T. Sawada, E. P. Shettle, *Photochem. Photobiol.* **19**, 251 (1974).
16. Supported by the U.S. Environmental Protection Agency, Stratospheric Impact Research and Assessment Program, grant R806489010. We thank A. E. S. Green and D. S. Nachtwey for helpful discussions.

15 August 1979; 2 January 1980

Cogeneration of Electric Energy and Nitric Oxide

Abstract. *A solid electrolyte fuel cell operating on ammonia fuel has been constructed and tested. The yield of nitric oxide can exceed 60 percent with simultaneous electric energy production. Two dimensionless numbers have been identified which govern the product selectivity and power output of this fuel cell. The cell appears to be a promising candidate for nitric acid and electric energy cogeneration.*

The oxidation of NH_3 to NO in a fuel cell has been a long-sought goal (*1*). It is a highly exothermic reaction with a Gibbs free energy ΔG of -64.5 kcal per mole of NH_3 at 1000 K, yet it is also the basic step for the industrial manufacture of HNO_3. [More than 6.8×10^6 tons of HNO_3 are produced annually in the United States alone (*2*).] A Pt-Rh alloy is used currently as the catalyst for the conversion of NH_3 to NO. Because of the high exothermicity of the reaction, large amounts of thermal energy are generated. It would be extremely desirable from an economic as well as an energy-conservation point of view to obtain this energy as electric rather than thermal energy.

Low- and medium-temperature NH_3 fuel cells have met with no success since N_2 was found to be the only oxidation product (*3*). High-temperature fuel cells operating on H_2 or CO fuel have been developed and tested (*4*).

We have found that the primary product of the high-temperature solid electrolyte fuel cell

$$NH_3,NO,N_2,Pt/ZrO_2$$
$$(8 \text{ percent } Y_2O_3)/Pt,air$$

0036-8075/80/0509-0593$00.50/0 Copyright © 1980 AAAS

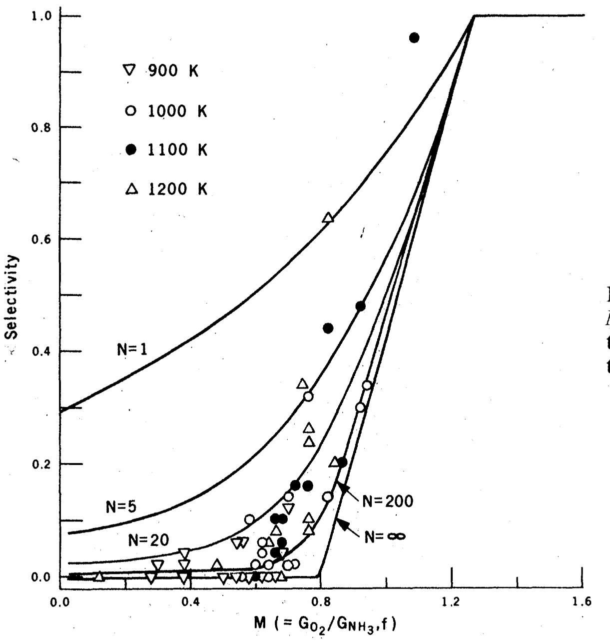

Fig. 1. Selectivity versus *M*. Solid lines correspond to kinetic model predictions (*5*).

operating at temperatures around 1100 K is NO, although significant amounts of by-product N_2 are also formed because of the catalytic reaction between NH_3 and NO on Pt. The influence of this side reaction can be minimized under optimal operating conditions.

The fuel cell consists of an 8 mole percent yttria-stabilized zirconia tube. Platinum electrodes were deposited on the inside and outside surfaces of the wall with Engelhard A-3788 Pt paste and calcining at 1300 K. The outside Pt electrode was exposed to ambient air. Ammonia diluted with He was allowed to flow continuously through the tube. The stabilized zirconia wall was fairly thick (~ 2 mm). The product composition of the fuel cell was monitored continuously by means of NH_3 and NO infrared analyzers. The NH_3 analyzer was also used for reactant analysis. A gas chromatograph was used periodically to check the results of the infrared analyzers. A Matheson certified NH_3 standard diluted with He was used as reactant. Pure He was also available to dilute the standard.

High selectivity to NO was obtained between 900 and 1200 K. Above 1200 K, the direct NH_3 decomposition to N_2 and H_2 becomes very fast. Using high NH_3 flow rates (*5*), we obtained power outputs of the order of 10^{-3} W per square centimeter of solid electrolyte. Under these conditions the selectivity to NO is very low, less than 5 percent. However, by decreasing the NH_3 molar flow rate, either by increasing the dilution or by increasing the residence time, we reached selectivities (moles of NO produced per mole of NH_3 reacted) of 97 and 64 percent at 24 and 82 percent conversions, respectively. Because of the very long residence time used, the power output dropped to 7 μW per square centimeter of electrolyte. The cell overpotential was shown to be almost entirely due to the ohmic resistance of the solid electrolyte. Therefore, the rate-limiting step for the anodic reaction is the diffusion of O^{2-} through the solid electrolyte.

Over the range of temperatures investigated, the selectivity depends critically (Fig. 1) on the dimensionless number *M* defined as

$$M = \frac{\text{Oxygen molar flux through electrolyte}}{\text{NH}_3\text{ molar flux through cell}} = \frac{G_{\mathrm{O_2}}}{G_{\mathrm{NH_3,f}}}$$

When $M < 0.75$, corresponding to the stoichiometric O_2/NH_3 ratio for N_2 formation, the selectivity is quite small, less than 5 percent. When $M > 0.75$, the selectivity to NO rises dramatically and can reach 97 percent for $M > 1$. This can be explained quantitatively (*5*) if the following two reactions take place at the anode

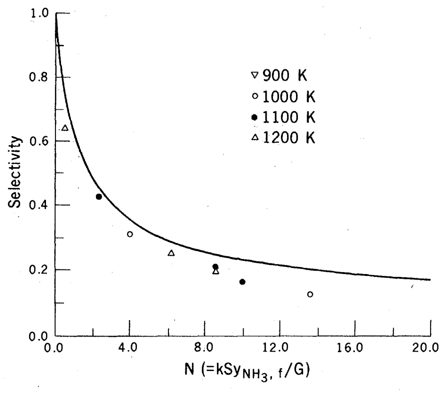

Fig. 2. Experimental and predicted selectivity versus *N* at $M = 0.75$.

$$2NH_3 + 5O^{2-} \rightarrow 2NO + 3H_2O + 10\ e^- \qquad (1)$$

$$2NH_3 + 3NO \xrightarrow{k} 5/2N_2 + 3H_2O \qquad (2)$$

and reaction 1 is rate limiting because of the slow diffusion of O^{2-} through the electrolyte. At constant *M* the selectivity is found, both experimentally (Fig. 2) and theoretically, to be uniquely determined by a second dimensionless number *N* defined as

$$N + kSy_{\mathrm{NH_3,f}}/G$$

where *k* is the rate constant for reaction 2 (assumed first-order in NH_3 and NO), *S* is the surface area of the anode, $Y_{\mathrm{NH_3,f}}$ is the mole fraction of NH_3 in the feed, and *G* is the total molar flow rate.

Since *M*, and therefore selectivity, is limited by the O^{2-} flux through the electrolyte, thinner electrolyte walls must be used to maintain high selectivity at higher NH_3 molar flow rates. This would also increase the power output proportionally to the reduction in the electrolyte wall thickness.

Improving the existing technology of thin stabilized zirconia film deposition on mechanically strong supports or using other highly conducting solid electrolytes can make the high-temperature NH_3 fuel cell a commercially attractive means for HNO_3 and electric energy cogeneration.

C. G. VAYENAS
R. D. FARR
Department of Chemical Engineering, Massachusetts Institute of Technology, Cambridge 02139

References and Notes

1. K. Denbigh, *The Principles of Chemical Equilibrium* (Cambridge Univ. Press, London, ed. 2, 1968), p. 76.
2. *Chem. Eng. News* **55**, 43 (June 1977).
3. R. O. Wynveen, in *Fuel Cells*, G. J. Young, Ed. (Reinhold, New York, 1963), vol. 2, chap. 12; M. Eisenberg, *Proc. Annu. Power Sources Conf.* **18**, 20 (1964).
4. D. H. Archer, J. J. Alles, W. A. English, L. Elikan, E. F. Sverdrup, R. L. Zahradnik, in *Fuel Cell Systems* (Advances in Chemistry Series 47, American Chemical Society, Washington, D.C., 1965), p. 332.
5. R. D. Farr, thesis, Massachusetts Institute of Technology (1979); D. Ortman, thesis, Massachusetts Institute of Technology (1979); C. Vayenas and R. D. Farr, *J. Electrochem. Soc.*, in press.
6. We thank D. Ortman, C. W. Cheng, and A. Ubel for their assistance in the early experiments. R.D.F. received financial support from the Massachusetts Institute of Technology, Energy Laboratory. This research was supported under grant ENG 77-27500 from the National Science Foundation.

15 October 1979; revised 11 January 1980